Edge effect on thermal transport in graphene nanoribbons: A phonon localization mechanism beyond edge roughness scattering

Yan Wang, Bo Qiu, and Xiulin Ruan[a)]
School of Mechanical Engineering and the Birck Nanotechnology Center, Purdue University, West Lafayette, Indiana 47907, USA

(Received 16 April 2012; accepted 12 June 2012; published online 2 July 2012)

Equilibrium molecular dynamics simulations show that graphene nanoribbons (GNRs) with zigzag edges have higher thermal conductivity (κ) than armchair-edged ones, and the difference diminishes with increasing temperature or ribbon width. The dominant phonon wavelength for thermal transport can be much longer (by orders of magnitude) than the difference between the "roughness" of smooth zigzag and armchair edges. Therefore, the roughness scattering theory is not sufficient to explain the largely different κ of GNRs with different edge chiralities. Cross-sectional decomposition of the steady-state heat flux shows significant suppression of thermal transport at edges, especially in armchair ones. This behavior is explored by phonon spectra analysis. Considerable phonon localization at edges is concluded to underlie the edge-chirality dependent κ of GNRs. © *2012 American Institute of Physics*. [http://dx.doi.org/10.1063/1.4732155]

Graphene has been recognized as a potential substitute for silicon in the electronics industry, mainly owing to its outstanding electronic and thermal properties.[1–5] The tunable band-gap opening and edge-chirality dependent electronic property of graphene nanoribbon (GNR), a narrow strip of graphene, makes the vast application of graphene-based devices even more promising.[1,6] GNR has also been predicted to have edge-chirality dependent thermal conductivity (κ), which was mostly predicted to be higher in zigzag-edged GNRs (zGNR) than armchair-edged ones (aGNR), i.e., $\Delta\kappa = \kappa_{zGNR} - \kappa_{aGNR} > 0$, though the underlying mechanism remains to be an open question.[4,7–10]

The notable difference between the topology of zigzag and armchair edges can lead people to attribute $\Delta\kappa$ to the surface/edge roughness scattering as usually seen in nanostructures.[10–13] As for thermal transport, the consideration of the surface/edge roughness scattering is usually meaningful only when the RMS height of the surface/edge variation (δ) is comparable to the dominant phonon wavelength (λ_{dom}) for carrying heat. For narrow GNRs, the thermal conductance (G) can be estimated by integrating the Landauer formula over the entire first Brillouin zone (FBZ) as[9,14]

$$G(T) = \int_{FBZ} \frac{v_g(k)}{2\pi} \Xi(k) \hbar\omega(k) \frac{\partial f^o(T)}{\partial T} dk, \tag{1}$$

where v_g, Ξ, $\hbar\omega$, and f^o are the group velocity, transmission probability, energy, and distribution of the phonons, respectively. We consider phonons with a sinusoidal dispersion, $\omega(k) = \omega_{max}\sin(ka/2)$, with a denoting the lattice constant of graphene (2.46 Å) and $\omega_{max} = 250$ THz the cutoff angular frequency.[15] The form of f^o depends on whether the system is quantum or classical[16] and Ξ is taken to be a constant. Figure 1 indicates that long wavelength phonons ($\lambda_{dom} \gtrsim 1$ nm) dominate thermal transport in GNRs. The wave nature of phonons indicates that it is beyond the resolution of those phonons with a λ much longer than the δ of the smooth edges of the GNRs ($\delta_{zGNR} \approx 0.2$ Å, $\delta_{aGNR} \approx 0.6$ Å) to distinguish their edge structure, and hence, edge roughness scattering should be excluded as the cause for the large $\Delta\kappa$ observed in previous studies using molecular dynamics (MD) or Green's function method.[4,9,17,18] A mechanism relatively independent to λ will be explored in this work.

It should be noted that previous MD studies on $\Delta\kappa$ mainly used non-equilibrium technique, which might suffer severe size effect due to the strong phonon–thermal bath scattering and the applied temperature bias induces extremely high temperature gradient and, hence, seriously inhomogeneous thermal strain in the nanosized simulation cells.[4,17,18] Unfortunately, the κ of GNR relies greatly on system length and strain,[18] and it is not clear whether these factors will affect the validity of those MD studies qualitatively. Herein, we use the LAMMPS package[19] to perform equilibrium MD simulations to calculate the κ of GNRs with the Green-Kubo method.[20,21] The optimized Tersoff potential parameters,[15] which are characterized by more accurate phonon dispersion and anharmonicity than the original set,[22] are used to model C-C interactions. The periodic boundary condition (bc) is applied to the length direction and free bc is used for the other two directions. κ is calculated from the longitudinal (subscript L) heat current autocorrelation function (HCACF) by

$$\kappa_{LL} = \frac{V}{k_B T^2} \int_0^\tau \langle J_L(\tau) J_L(0) \rangle d\tau, \tag{2}$$

where V and T are the volume and temperature of the GNR, and k_B is the Boltzmann constant. The full heat current vector $\vec{J}$ is computed as[23]

$$\vec{J}(t) = \frac{1}{V}\left\{ \sum_i \vec{v}_i \epsilon_i + \frac{1}{2} \sum_{i,j,i\neq j} \vec{r}_{ij} (\vec{F}_{ij} \cdot \vec{v}_i) + \sum_{i,j,k} \vec{r}_{ij} [\vec{F}_j(ijk) \cdot \vec{v}_j] \right\}, \tag{3}$$

a)E-mail: ruan@purdue.edu.

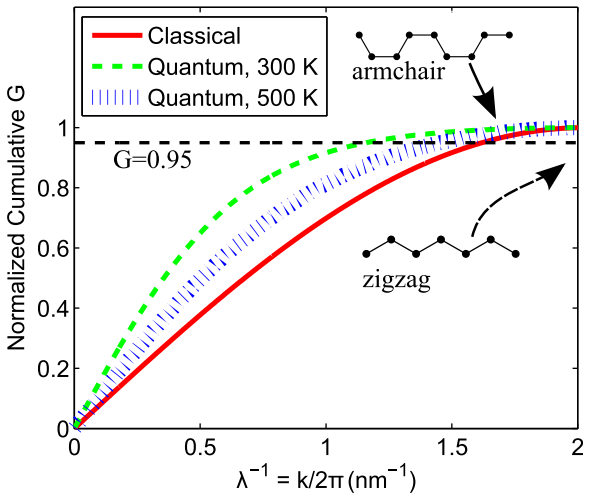

FIG. 1. Normalized cumulative thermal conductance (G) as a function of the reciprocal phonon wavelength, $\lambda^{-1} = k/2\pi$.

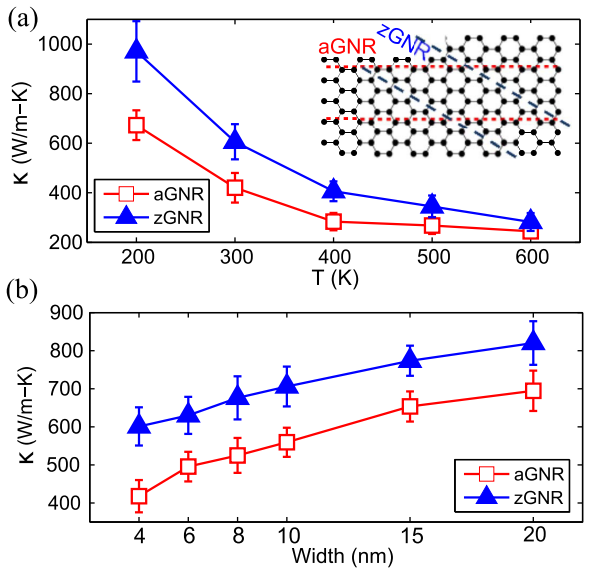

FIG. 2. (a) and (b) The κ of aGNRs and zGNRs at different T (width = 4 nm) and for different GNR widths ($T = 300$ K). 15 independent simulations are performed to account for the statistical fluctuation of the MD results. The inset shows how aGNR and zGNR are cut from graphene.

where $\vec{v}$ and ϵ denote the velocity and energy of the atom i, and $\vec{r}$ and $\vec{F}$ are the distance and the two/three-body interaction between different atoms (i, j, or k). The GNR is first relaxed at zero pressure and prescribed temperature via the Nosé-Hoover thermostat[24,25] for 0.8 ns (0.4 fs/step). Then it is switched into the NVE ensemble for another 10.8 ns of which the last 10 ns are used to calculate the HCACF. We have found that an autocorrelation (AC) length shorter than 5 ns can result in largely inaccurate results, thus a sufficiently long AC length is crucial for the validity of this method.[26] We have also checked the length (l) dependence of κ, and a saturating trend starts when $l > 6.0$ nm but longer l suffers much less statistical fluctuation. A system length of 15 nm is used for all simulations in this work. This method does not need thermal bath during the data production process, resulting in much less phonon–thermal bath scattering and thermal strain inhomogeneity, which is advantageous to previous MD works.[4,17,18]

We compare the κ of aGNRs and zGNRs in Fig. 2. As shown in Fig. 2(a), both κ_{aGNR} and κ_{zGNR} decrease with T, while the latter is always higher. The T dependence is mainly due to the enhanced Umklapp scattering, and it affects zGNR more strongly than aGNR so that the κ of them eventually becomes the same at temperatures higher than 600 K, when Umklapp scattering dominates. These results agree qualitatively with previous MD simulations,[17,18] though they obtained lower κ due to the size effect or the different interatomic potential used. Figure 2(b) shows that κ increases with width for both types of GNRs. The κ of bulk graphene is also computed by applying the periodic bc to the width direction, and the values are essentially the same for the zigzag and armchair directions (~1200 W/m-K) at 300 K. This indicates that the presence of edges in GNR breaks the isotropy of κ of bulk graphene, endowing it with chirality and width dependence.

Noting that Eq. (3) can be used to compute the local heat flux vector for a specific group of atoms, we calculate the cross-sectional distribution of the longitudinal heat flux in GNRs, i.e., α = Local J/Total J. As shown in the inset of Fig. 3, the cross-section of a GNR is uniformly divided into eight columns, and a constant heat flux (1.0 eV/ps) is added to or subtracted from either end by directly rescaling the kinetic energy to establish a steady-state heat conduction condition with constant heat flow. The α for aGNRs and zGNRs is plotted in Fig. 3, and we note that the heat flow near edges is significantly suppressed, especially in aGNRs. Similar phenomenon has been reported in Si/Ge core-shell nanowires, Si nanowires, and nanotubes, where phonon localization was found to suppress the heat transport near the surface of the nanowire or nanotube greatly.[23,27] Here, our results suggest that smooth edges in nanoscale 2D materials can also play a crucial role in thermal transport.

To further explore the underlying mechanism, we calculate the phonon vibrational density of states (vDOS)[23] and the phonon participation ratio (p).[28] The former is calculated from the Fourier transform of the velocity-velocity AC

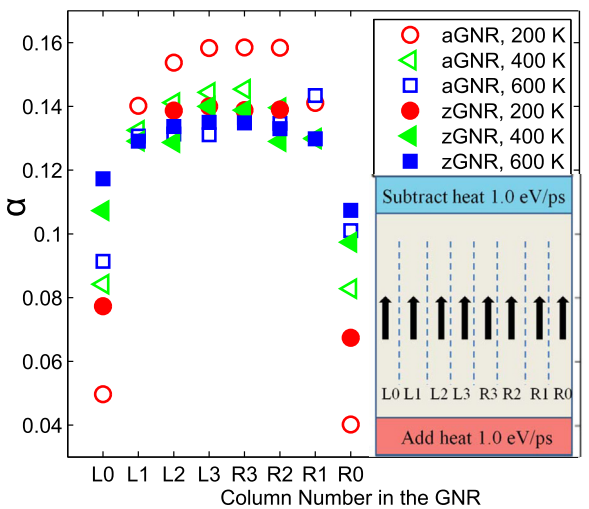

FIG. 3. Cross-sectional heat flux distribution in aGNRs and zGNRs at various temperatures. The inset shows the simulation domain setup for these calculations.

functions, and the latter, defined for each eigen-mode (γ), is computed as

$$p_\gamma^{-1} = N\sum_i \left(\sum_\xi \epsilon^*_{i\xi,\gamma}\epsilon_{i\xi,\gamma}\right)^2, \quad (4)$$

where $\epsilon_{i\xi,\gamma}$ is the eigen-vector component of the γth normal mode of the lattice vibration in polarization ξ (x, y, or z), and i sums over all the atoms of interest. We use the superposed $*$ symbol to denote complex conjugate in this work. By definition, $p_\gamma = 1$ if the γth mode is completely delocalized and $p_\gamma = 1/N$ for complete localization. As shown in Fig. 4(a), the vDOS is almost the same for bulk graphene, aGNR and zGNR at most frequencies except strong peaks or valleys present in both aGNR and zGNR while absent in bulk graphene near the center and the tail of the vDOS. Figure 4(b) shows that these modes are localized, which cannot transport thermal energy as efficiently as the delocalized ones.[23,28]

Based on Eq. (4), we can evaluate the spatial distribution of eigen-modes in a specific range, $\Gamma = \{\gamma : p_\gamma < p_c\}$, by

$$\Phi_{\xi,\Gamma}(i) = \frac{\sum_{\gamma\in\Gamma}\epsilon^*_{i\xi,\gamma}\epsilon_{i\xi,\gamma}}{\sum_j\sum_{\gamma\in\Gamma}\epsilon^*_{j\xi,\gamma}\epsilon_{j\xi,\gamma}}, \quad (5)$$

where p_c denotes a criteria for localization. In Fig. 4(c), we plot the $\Phi_{\xi=z}$ for the modes within $\Gamma = \{\gamma : p_\gamma < 0.4\}$ for aGNR and zGNRs, and $\Gamma = \Gamma_{aGNR} \cup \Gamma_{zGNR}$ for graphene, where a large value of Φ indicates a high concentration of the corresponding set of eigen-modes at atom i. It is obvious that the localized modes indicated in Fig. 4(b) are localized on the edges of GNRs and are stronger in aGNR than in zGNR. Moreover, the magnitude of Φ decreases exponentially with the distance to edges, which results in less suppression of thermal transport in the central region of GNRs.

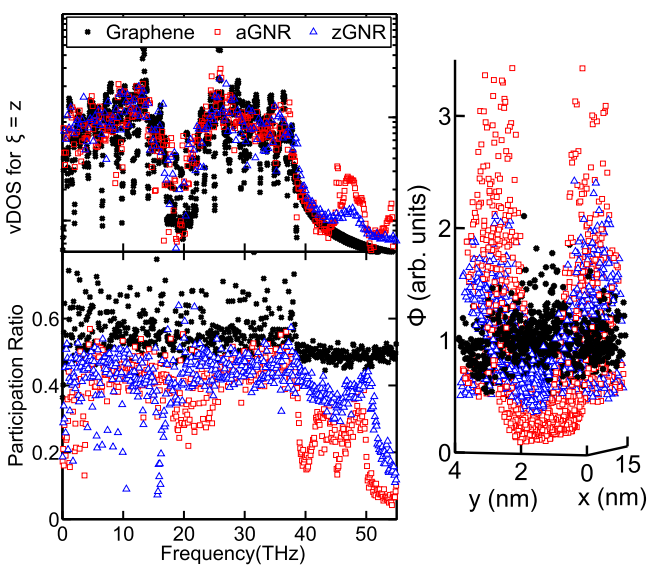

FIG. 4. (a) and (b) The vDOS and the phonon participation ratio of a bulk graphene, aGNR, and zGNR. (c) The spatial distribution (Φ) of modes within $\Gamma = \{\gamma : p_\gamma < 0.4\}$ for aGNR and zGNRs, and $\Gamma = \Gamma_{aGNR} \cup \Gamma_{zGNR}$ for graphene. The height in (c) corresponds to the magnitude of localization at that position (x,y).

These phonon spectra analyses combined with the non-uniform heat flux distribution shown in Fig. 3 indicate that the strong edge localization of phonons suppresses thermal transport in GNRs greatly and is responsible for the $\Delta\kappa$ between aGNR and zGNR. Besides, localized modes can induce inelastic phonon scatterings at the boundary, which reduces κ if the interaction is anharmonic.[29,30]

To summarize, we conducted equilibrium MD simulations with the optimized Tersoff potential and confirmed that κ of zGNRs is higher than that of aGNRs with the same width at a wide range of temperature, though κ was found to be the same for the zigzag and armchair directions in bulk graphene. Edge roughness scattering should be excluded as the reason for such phenomenon, since the dominant phonon wavelength estimated from the Landauer formula can be orders of magnitude longer than the difference between the δ of smooth zigzag and armchair edges, and hence, it lacks the resolving power to distinguish between them. By decomposing the heat flux along the width direction of a GNR, we observed strong suppression of thermal transport at edges. Analyses on the vDOS and the participation ratio revealed strong localization of phonons in regions near and at the edges of GNRs, especially aGNRs, which suppresses thermal transport. Besides, the enhanced phonon scattering by those localized modes can further reduce κ. Our work revealed the importance of edges to thermal transport in GNRs and indicates an efficient way to tune the thermal property of 2D materials by engineering the edges.

The authors thank the support from the Air Force Office of Scientific Research (Grant No. FA9550-11-1-0057) and the Purdue Network for Computational Nanotechnology (NCN).

[1]A. K. Geim and K. S. Novoselov, Nature Mater. **6**, 1476–1122 (2007).
[2]A. A. Balandin, S. Ghosh, W. Bao, I. Calizo, D. Teweldebrhan, F. Miao, and C. N. Lau, Nano Lett. **8**, 902 (2008).
[3]A. A. Balandin, Nature Mater. **10**, 569 (2011).
[4]J. Hu, X. Ruan, and Y. P. Chen, Nano Lett. **9**, 2730 (2009).
[5]J. Haskins, A. Kinaci, C. Sevik, H. Sevinçi, G. Cuniberti, and T. Çğin, ACS Nano **5**, 3779 (2011).
[6]K. Nakada, M. Fujita, G. Dresselhaus, and M. S. Dresselhaus, Phys. Rev. B **54**, 17954 (1996).
[7]Z. Aksamija and I. Knezevic, Appl. Phys. Lett. **98**, 141919 (2011).
[8]Y. Xu, X. Chen, B.-L. Gu, and W. Duan, Appl. Phys. Lett. **95**, 233116 (2009).
[9]Z. W. Tan, J.-S. Wang, and C. K. Gan, Nano Lett. **11**, 214 (2011).
[10]W. J. Evans, L. Hu, and P. Keblinski, Appl. Phys. Lett. **96**, 203112 (2010).
[11]L. Liu and X. Chen, J. Appl. Phys. **107**, 033501 (2010).
[12]B. Qiu, L. Sun, and X. Ruan, Phys. Rev. B **83**, 035312 (2011).
[13]P. Martin, Z. Aksamija, E. Pop, and U. Ravaioli, Phys. Rev. Lett. **102**, 125503 (2009).
[14]Z. Huang, T. S. Fisher, and J. Y. Murthy, J. Appl. Phys. **108**, 094319 (2010).
[15]L. Lindsay and D. A. Broido, Phys. Rev. B **81**, 205441 (2010).
[16]J. E. Turney, A. J. H. McGaughey, and C. H. Amon, Phys. Rev. B **79**, 224305 (2009).
[17]H.-Y. Cao, Z.-X. Guo, H. Xiang, and X.-G. Gong, Phys. Lett. A **376**, 525 (2012).
[18]Z. Guo, D. Zhang, and X.-G. Gong, Appl. Phys. Lett. **95**, 163103 (2009).
[19]S. Plimpton, J. Comput. Phys. **117**, 1 (1995).
[20]P. K. Schelling, S. R. Phillpot, and P. Keblinski, Phys. Rev. B **65**, 144306 (2002).
[21]K. Esfarjani, G. Chen, and H. T. Stokes, Phys. Rev. B **84**, 085204 (2011).
[22]J. Tersoff, Phys. Rev. B **37**, 6991 (1988).
[23]M. Hu, K. P. Giapis, J. V. Goicochea, X. Zhang, and D. Poulikakos, Nano Lett. **11**, 618 (2011).
[24]S. Nosé, J. Chem. Phys. **81**, 511 (1984).

[25]W. G. Hoover, Phys. Rev. A **31**, 1695 (1985).
[26]See supplementary material at http://dx.doi.org/10.1063/1.4732155 for the details of how to determine appropriate parameters for equilibrium molecular dynamics simulations using the Green-Kubo method.
[27]J. Chen, G. Zhang, and B. Li, Nano Lett. **10**, 3978 (2010).
[28]A. Bodapati, P. K. Schelling, S. R. Phillpot, and P. Keblinski, Phys. Rev. B **74**, 245207 (2006).
[29]M. Wagner, Phys. Rev. **131**, 1443 (1963).
[30]S.-K. Chien, Y.-T. Yang, and C.-K. Chen, Appl. Phys. Lett. **98**, 033107 (2011).